

Distortion Prediction in Selective Laser Melting: Methodology for Inherent Strain Determination

Iñaki Setien¹, Maria San Sebastian¹, Alberto Echeverría¹

¹ IK4-LORTEK, Technological Centre, Arranomendia kalea, 4A, Ordizia 20240 (Spain)

* Corresponding Author: isetien@lortek.es, +34 943 88 23 03

Abstract

One of the process variants in metal additive manufacturing (AM) is the Selective Laser Melting (SLM) where parts are built on a layer by layer basis. A focused power source is applied (laser or electron beam) to the powder material which is rapidly heated above its melting temperature and then allowed to solidify and cool down to form a new solid layer. Typically, this manufacturing process induces residual stresses and distortions. Distortions are critical since they increase manufacturing costs, times and generate wastes and scraps due to dimensional inaccuracies. Therefore, a priori prediction of these distortions at design stage is preferred to trial and error strategy usually employed.

The detailed transient thermo-mechanical analysis (DTA) is commonly considered as the reference modelling strategy for AM processes. Nevertheless, the use of simplified methodologies, such as the Inherent Strain Method, is required in order to overcome the large computational cost needed by the DTA.

This work copes with the analysis, development and application of the Inherent Strain Method for the prediction of the final distortions in powder bed based SLM process. The main objective is to assess the predictive capability of this simplified model based on the inherent strain calibration strategy developed for that purpose. The assessment has been conducted correlating numerical results and experimental measurements in some testing geometries.

1 Introduction

Additive Manufacturing (AM) gathers various techniques for building three dimensional objects on a layer by layer sequence. The Selective Laser Melting (SLM) is one of the most widespread powder-bed based technology for metallic components.

In these processes, the material is locally and rapidly heated and then allowed to solidify in order to form a dense geometry. This involves large thermal strains generating residual stress and distortion [1]. This article is focused on the post-build part distortion originated by the SLM process.

Post-build part distortion is a critical issue during AM of metallic parts since it prevents the technology from being implemented at industrial level. This phenomenon increases manufacturing costs and generates waste and scrap due to the dimensional inaccuracies between the nominal and built geometries.

Currently, corrective solutions are often taken based on trial and error approach in order to avoid the aforementioned issues. This implies several builds until the correct part is achieved, usually being a tedious task.

In this regard, Design Against Distortion (DAD) paradigm arises which is focused on the development of numerical modelling methodologies to anticipate distortion problems even from the design stage. However, this new paradigm requires the development of new modelling strategies efficient enough to be applied to real parts.

AM physical fundamentals are very similar to those of multi-pass welding processes. Therefore, Finite Element Method (FEM) based welding modelling techniques developed so far can be adapted to develop AM simulations [2]–[4]. However, added difficulties such as longer process time, higher number of passes, much more deposited material, ... must be considered.

Regarding these FEM strategies, detailed transient thermo-mechanical models have already been successfully applied and validated in order to predict thermal and mechanical behaviour of AM processes [5]–[10]. Nevertheless, these high-fidelity modelling approaches are only feasible at meso-scale level due to the computational time limitations. Indeed, this computational demand prevents this approach from being applied to real parts in order to predict thermal and mechanical history.

Therefore, several simplified methodologies have been developed in order to model this process at large scale level [5], [11], [12]. One of the most promising and efficient simplified approach is the inherent strain method [13], [14]. This well-known methodology has already been successfully applied to both Computational Welding Mechanics (CWM) and AM processes. This allows replacing computationally costly thermo-mechanical simulations by a mechanical faster one. As a result, the way these characteristic inherent strains are obtained is the key point in this simplified methodology.

The work presented in this paper is focused on the development of an experimental test based methodology

to determine characteristic inherent strains. In addition, the validation of this methodology has been conducted applying it at coupon level (twin-cantilever geometry) and comparing numerical and experimental distortion results.

2 Numerical model development

2.1 Inherent strain method

The inherent strain method was first developed by the team led by Ueda [13]. Basically, the method states that if characteristic inherent strain field is known beforehand, an elastic linear FE analysis is enough to predict the distortion field of a given structure (see Figure 1).

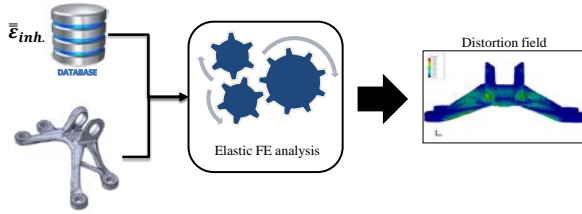


Figure 1: inherent strain methodology illustration.

The application of the inherent strain method to AM simulations is carried out in a macroscopic layer level. Hence, the whole part is partitioned in simulation layers which may represent one or several real layers. In this way, each simulation layer is activated sequentially and applied the corresponding inherent strain field until the whole geometry is achieved. This evolution can be observed in Figure 2.

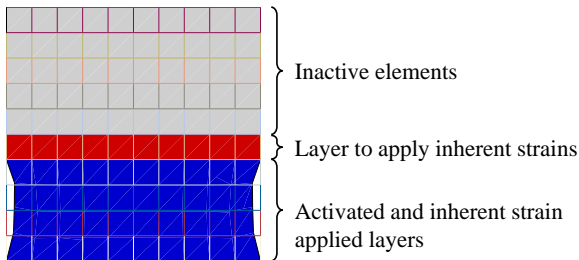


Figure 2: inherent strain application sequence.

The element and layer activation strategy is based on the so called “birth and death” or “inactive element method” technique. According to this activation strategy, elements are not part of the model until they are activated [15]. The nominal height based powder feeding intrinsic to the Powder Bed Deposition (PBD) processes is modelled adequately by means of this activation strategy.

The geometry is meshed with a layer wise FEM mesh where the interface nodes are placed on a flat surface.

2.2 Inherent strain determination

As pointed out in the introduction, the key factor of the inherent strain methodology is to know beforehand the inherent strain tensor. Actually, this is the main driving force which induces strains layer by layer prompting to distortion and residual stress.

Two methods can be distinguished for this purpose:

- High-fidelity thermo-mechanical FEM models based methodology.
- Experimental test results based methodology.

This paper will focus on the second method, the one based on experimental tests. With this in mind, in the following lines this methodology will be described.

To begin with, two principal assumptions are made. In the first place, the inherent strain tensor is considered to be orthogonal (1). In like manner, another assumption is made neglecting the tensor’s component in the building direction (2).

$$\varepsilon^{inh} \rightarrow \text{orthogonal} \quad (1)$$

$$\varepsilon_{ww}^{inh} = 0 \quad (2)$$

In this way, this methodology consists of an iterative fitting loop. Certainly, the inherent strain tensor components are calculated so that the FEM model previously described is able to predict the same distortion behaviour as the experimental tests.

The fitting process can be described by the following steps:

Step 1: manufacturing of real coupons

Twin-cantilever beams (see geometry in Figure 3) are manufactured following three different scanning strategies: longitudinal, transversal and 45° stripes (see Figure 4). From layer to layer, scanning strategy is kept constant.

After manufacturing, specimens are partially cut from the baseplate by wire cutting (w-EDM), leaving the middle column attached to the baseplate. Thus, the residual stress field cumulated during the manufacturing process is redistributed leading to the bowing of the part. Then, the vertical distortion field is measured on the top surface as can be observed in Figure 5.

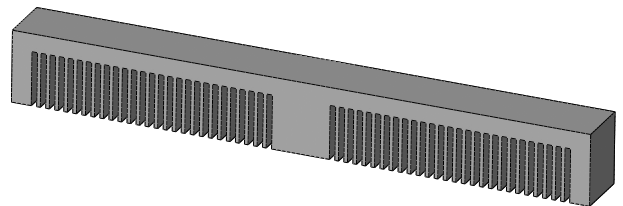


Figure 3: twin-cantilever beam geometry.

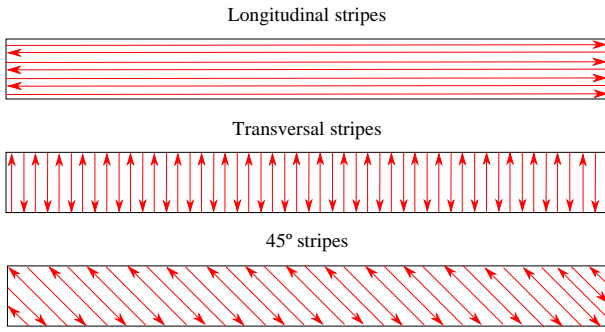


Figure 4: scanning strategies for twin-cantilevers.

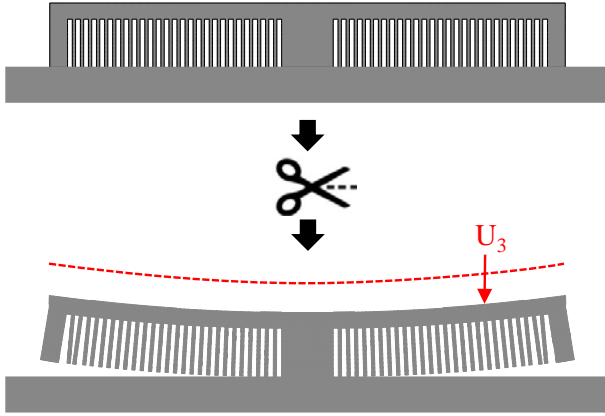


Figure 5: twin-cantilever cutting and vertical distortion measurement.

Step 2: iterative inherent strain fitting process

Once the distortion field is known for each scanning strategy, the process continues with step 2. On account of a data matching algorithm depicted in Figure 6, in-plane inherent strain values are calculated. The algorithm changes both inherent strain components (ϵ_{uu}^{inh} and ϵ_{vv}^{inh}) until the vertical distortion curve fits with experimental results within a predetermined error.

As far as the loop is concerned, two FEM simulations are conducted simultaneously in each loop: one for the longitudinal stripes inherent strain simulation and the other for the transversal stripes strategy. In addition, the loop is also fed up with experimental results obtained in step 1.

Step 3: results checking

Finally, a checking is carried out based on the 45° stripes experimental results. Basically, taking the inherent strain tensor calculated in Step 2, a FEM simulation is conducted for 45° stripes test case. Hence, the predicted distortion field is compared with the experimental result. In this way, the fitting process validity is checked.

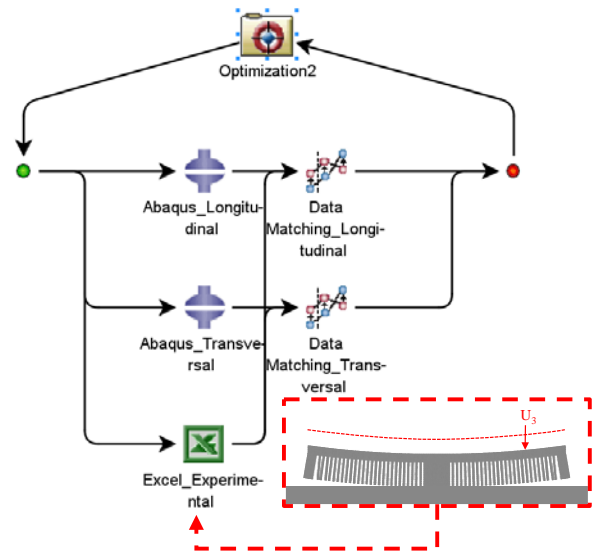


Figure 6: data matching iterative loop.

3 Methodology application

This section describes the application of the methodology set up in the previous section.

3.1 Step 1: twin-cantilever beams manufacturing and distortion results

Following the aforementioned inherent strain determination strategy, the first step was the manufacturing of twin-cantilevers following three different scanning strategies.

The specimens were made of Ti-6Al-4V and they were manufactured in a SLM 250 (from MCP-Realizer) with 200 W fibre laser. 50 μm layer thickness was used together with the process parameters summarised in Table 1.

All specimens were manufactured in two baseplates and were partially cut from the baseplate (see Table 2) as indicated in the previous section. To finish with the first step, vertical distortions were measured on the top surface along the beam length.

In the graph shown in Figure 7, the normalised vertical distortion results can be observed taken as reference the longitudinal stripes results. In this regard, a clear influence of scanning strategies can be noticed. Longitudinal stripes lead to the highest distortions whereas transversal stripes to the reduced ones. Meanwhile, 45° stripes' results are between the previous ones. It is also remarkable the fact that 45° stripes distortion magnitude is the arithmetic mean of the longitudinal and transversal distortion fields.

Table 1: SLM process parameters.

| | Hatch | Boundary |
|----------------------------------|-------|----------|
| Laser power (W) | 200 | 150 |
| Scanning speed (mm/s) | 950 | 830 |
| Hatch distance (μm) | 120 | - |

Table 2: manufactured twin-cantilever beams before and after w-EDM process.

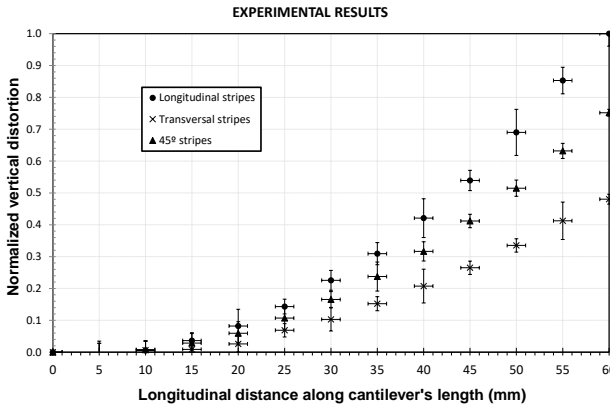
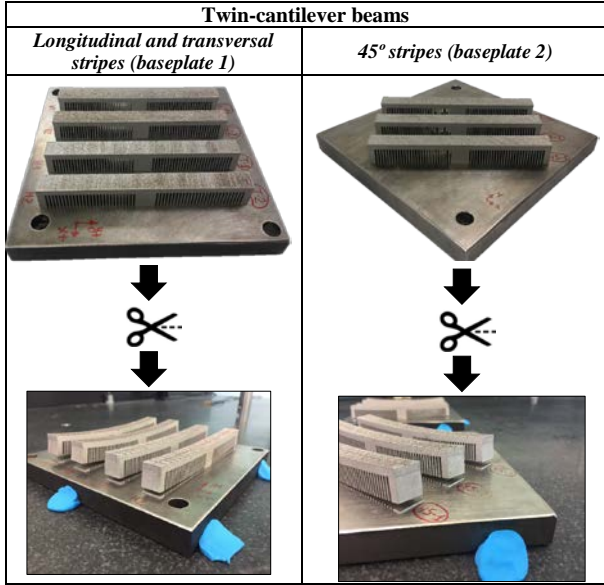


Figure 7: experimental normalized vertical distortions along twin-cantilever's half length.

3.2 Step 2: iterative inherent strain fitting

After the iterative process, the normalised inherent strain tensor can be seen in (3).

$$\bar{\epsilon}^{inh} = \begin{bmatrix} -1 & 0 & 0 \\ 0 & -0.33 & 0 \\ 0 & 0 & 0 \end{bmatrix} \quad (3)$$

The vertical distortion field obtained by FEM, taking as input data the above inherent strain, can be observed in Figure 8 and Figure 9. In the same way, the vertical

distortion curves on top of the twin cantilever (Figure 10 and Figure 11) show how the data matching algorithm fits both curves to the provided experimental results.

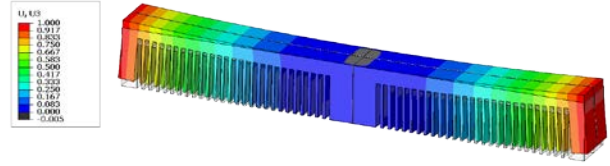


Figure 8: normalised vertical distortion field (scaled $\times 2$). Longitudinal stripes twin-cantilever.

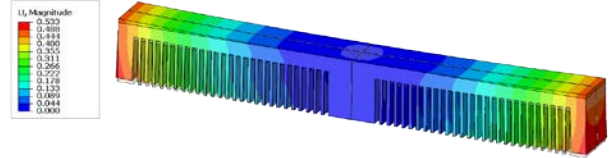


Figure 9: normalised vertical distortion field (scaled $\times 2$). Transversal stripes twin-cantilever.

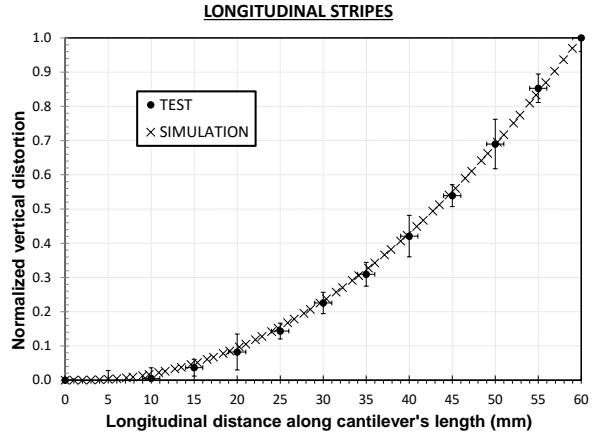


Figure 10: longitudinal stripes twin-cantilever. Normalised vertical distortion on the top surface.

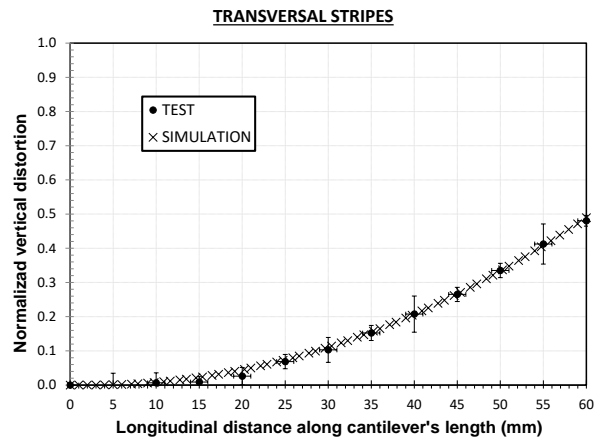


Figure 11: transversal stripes twin-cantilever. Normalised vertical distortion on the top surface.

3.3 Step 3: checking

To conclude with the process, the final checking step was conducted. Hence, the tensor (3) was introduced to the 45° FEM model obtaining the vertical distortion field plotted in Figure 12. In this regard, Figure 13 shows the clearest evidence of the validity of the inherent strain tensor through the good agreement between experimental and FEM results.

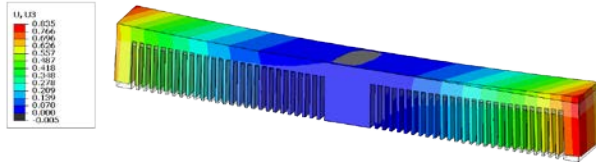


Figure 12: normalised vertical distortion field (scaled $\times 2$). 45° stripes twin-cantilever.

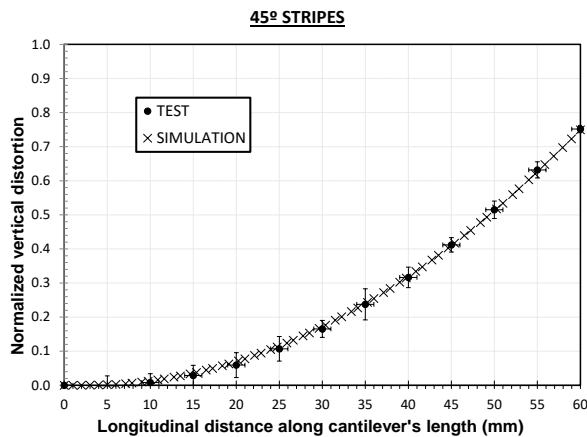


Figure 13: 45° stripes twin-cantilever. Normalised vertical distortion on the top surface.

4 Conclusions

An inherent strain calibration methodology based on experimental tests has been defined. Hence, inherent strain methodology based simplified models can be used for distortion prediction as long as the inherent strain tensor is known or calculated.

The suitability of this inherent strain calculation method has been proven at coupon level.

The following practical conclusion can be drawn:

- Experimental distortions clearly depend on the scanning strategy.
- Orthogonal nature of inherent strains has been observed.
- Experimental test based inherent strain determination methodology seems to be a valid option. Then again, its validity should also be checked in other more complex geometries where there is no any stress relaxation due to the cutting process.

Acknowledgements

The work forms part of the DISTRACTION project, funded by the European Union's Horizon 2020 research and innovation programme under Grant Agreement No. 686808. The authors would like to thank Airbus Structures Research, especially Sjoerd van der Veen, for his valuable contributions.

Literature

- [1] J. P. Kruth, L. Froyen, J. Van Vaerenbergh, P. Mercelis, M. Rombouts, and B. Lauwers, "Selective laser melting of iron-based powder," *J. Mater. Process. Technol.*, vol. 149, no. 1, pp. 616–622, 2004.
- [2] P. Michaleris, *Minimization of welding distortion and buckling*. Woodhead Publishing Limited, 2011.
- [3] J. A. Goldak and M. Akhlaghi, *Computational welding mechanics*. Springer Science & Business Media, 2006.
- [4] L.-E. Lindgren, *Computational welding mechanics*. Elsevier, 2014.
- [5] L. Papadakis, A. Loizou, J. Risse, and J. Schrage, "Numerical Computation of Component Shape Distortion Manufactured by Selective Laser Melting," *Procedia CIRP*, vol. 18, pp. 90–95, 2014.
- [6] E. R. Denlinger, M. Gouge, J. Irwin, and P. Michaleris, "Thermomechanical model development and in situ experimental validation of the Laser Powder-Bed Fusion process," *Addit. Manuf.*, vol. 16, pp. 73–80, 2017.
- [7] L.-E. Lindgren, A. Lundbäck, M. Fisk, R. Pederson, and J. Andersson, "Simulation of additive manufacturing using coupled constitutive and microstructure models," *Addit. Manuf.*, May 2016.
- [8] M. Chiumenti, E. Neiva, E. Salsi, M. Cervera, S. Badia, J. Moya, Z. Chen, C. Lee, and C. Davies, "Numerical modelling and experimental validation in Selective Laser Melting," *Addit. Manuf.*, vol. 18, no. Supplement C, pp. 171–185, 2017.
- [9] C. Li, J. F. Liu, and Y. B. Guo, "Prediction of Residual Stress and Part Distortion in Selective Laser Melting," *Procedia {CIRP}*, vol. 45, pp. 171–174, 2016.
- [10] D. Pal and B. Stucker, "A New and Efficient Multi-Scale Simulation Architecture for the Prediction of Performance Metrics of Parts Fabricated Using Additive Manufacturing," *TMS2015*, 2015.
- [11] T. A. Krol, S. Westhäuser, M. F. Zäh, J. Schilp, and G. Groth, "Development of a Simulation-Based Process Chain – Strategy for Different

- Levels of Detail for the Preprocessing Definitions,” vol. 21, pp. 135–140, 2011.
- [12] N. Keller, F. Neugebauer, H. Xu, and V. Ploshikhin, “Thermo-mechanical Simulation of Additive Layer Manufacturing of Titanium Aerospace structures,” no. figure 1, 2013.
- [13] Y. Ueda, H. Murakawa, K. Nakacho, and N. X. Ma, “Establishment of computational welding mechanics,” *Weld. Surf. Rev.*, vol. 8, no. 1, pp. 265–299, 1997.
- [14] H. Murakawa, Y. Luo, and Y. Ueda, “Inherent strain as an interface between computational welding mechanics and its industrial application,” *BOOK-INSTITUTE Mater.*, vol. 695, pp. 597–619, 1998.
- [15] A. Lundbäck, “Modelling and simulation of welding and metal deposition,” Luleåtekniska universitet, 2010.